Environmental Pollution 315 (2022) 120347

Contents lists available at ScienceDirect

Environmental Pollution

journal homepage: www.elsevier.com/locate/envpol

Chemistry, transport, emission, and shading effects on NO_2 and O_x distributions within urban canyons

Yuqing Dai, Xiaoming Cai, Jian Zhong, Andrea Mazzeo, A. Rob MacKenzie *

School of Geography, Earth & Environmental Sciences, University of Birmingham, Edgbaston, Birmingham, B15 2TT, UK

ARTICLE INFO

Keywords:
Shading effects
Air pollution
MBM-FleX
Photochemistry
VOCs

ABSTRACT

The capacity to predict NO_2 and the total oxidant ($O_x = NO_2 + O_3$) within street canyons is critical for the assessment of air quality regulations aimed at enhancing human wellbeing in urban hotspots. However, such assessment requires the coupling of numerous processes at the street-scale, such as vehicular emissions and tightly coupled transport and photochemical processes. Photochemistry, in particular, is often ignored, heavily simplified, or parameterized. In this study, MBM-FleX — a process-based street canyon model that allows fast computation of various emission profiles and sun-lit conditions with tightly coupled physical (transport and mixing) and chemical processes and without loss of sufficient spatial resolution — was used to simulate shading effects on reactive species within urban canyons. Driven by pre-generated large-eddy simulation of flow, MBM-FleX results show that shading effects on volatile organic compound (VOC) free-radicals significantly affect the interconversion of odd-oxygen species that cannot be captured by the simple NO_x-O_3 chemistry, for example, reducing NO_2 by limiting the formation of hydroperoxyl radicals. Consistent with previous results in simpler model systems, the inclusion of VOC free-radical chemistry did not appreciably alter the sensitivity of NO_2 to shading intensity in regular canyons, but a non-linear relationship between NO_2 and shading intensity is found in deep canyons when the air residence time grew. When solar incidence simultaneously passes through multiple vortices in street canyons, VOC chemistry and shade may considerably influence model results, which may therefore affect the development of urban planning strategies and personal exposure evaluation.

1. Introduction

Urban air pollution is critically important to human wellbeing given that the urban population is expected to grow rapidly to 68% in the world by 2050 (Nations, 2018) and human exposure to air pollution can lead to increases in respiratory morbidity and mortality (Anenberg et al., 2018; Murray et al., 2020; Zeng et al., 2020). For instance, nitrogen dioxide (NO_2) is a vital contributor to urban air pollution as a gaseous pollutant and as a precursor to aerosol formation, and its concentration can become high in some urban "hotspots" such as street canyons, which describe a narrow street flanked by continuous obstructions on both sides, forming a stagnant environment with, in general, heavy emissions and reduced dispersion. Street canyons are becoming increasingly prevalent as urban areas grow denser (Joint Air Quality Unit, 2017). They can be categorized into three groups based on their aspect ratios (AR, defined as the ratio of canyon height to street width): avenue canyons with AR $\leq$ 0.5; regular canyons with AR $\approx$ 1.0 and no significant openings on the facade; and deep canyons with AR $\geq$ 2.0 (Vardoulakis et al., 2003). The characteristic of airflow and dispersion pattern within urban canyons are sensitive to Reynolds number (Re) (Chew et al., 2018), roof shape (Takano and Moonen, 2013), in-canyon trees and green infrastructure (Abhijith et al., 2017; Gromke and Ruck, 2007; Yazid et al., 2014), street orientation, and ARs (Ahmad et al., 2005; Chatzidimitriou and Yannas, 2017). The ventilation of canyons generally decreases with increased ARs, leading to poorer air quality at the pedestrian level and hence serious public health consequences for citizens exposed to such circumstances (Solazzo et al., 2011).

Nitrogen oxides (NO_x, a summation of the nitrogen oxides NO and NO_2) and ozone (O_3) undergo closely coupled dynamics and chemical processes within the urban canyon environment (Garmory et al., 2009), which have motivated research studies. Salmond et al. (2013) conducted a field monitoring campaign and suggested that the presence of leaves on trees would resist vehicular emissions moving upward to the rooftop along the leeward facade, giving marked impacts on in-canyon dynamics

* Corresponding author.
E-mail addresses: yxd598@bham.ac.uk (Y. Dai), x.cai@bham.ac.uk (X. Cai), j.zhong.1@bham.ac.uk (J. Zhong), mazzeo@bham.ac.uk (A. Mazzeo), a.r.mackenzie@bham.ac.uk (A.R. MacKenzie).

https://doi.org/10.1016/j.envpol.2022.120347
Received 11 July 2022; Received in revised form 24 September 2022; Accepted 29 September 2022
Available online 3 October 2022

and chemistry. A variety of parametric (e.g. canyon box models) and numerical (e.g. Computational fluid dynamics (CFD)) models integrated with chemical schemes have been used to simulate the behavior of air pollutants (e.g. temporal and spatial distributions, mass exchanges with the overlying background) within street canyons (Bright et al., 2013; Kim et al., 2012; Kwak and Baik, 2012; Wu et al., 2021; Zhong et al., 2016a, 2017). Particles in street canyons raised similar issue of transport and aerosol microphysics (e.g. Zhong et al. (2018)). However, most of these studies hypothesized constant photolysis rates within street canyons primarily due to expensive computational cost in numerical models. Given that the photolysis rate of NO_2 can be 20–40% of the theoretical value on overcast (Finlayson-Pitts and Pitts Jr, 1999) or hazy (Li et al., 2018) days, our knowledge of shading effects on air pollution within street canyons remain limited.

Although CFD-based air quality models offer the most convincing physical simulations based on current understanding, they require enormous computational resources in general, which increases by several orders of magnitude when complex volatile organic compound (VOC) free-radical schemes are involved. Hence, many earlier simulations either employed simple NO_x-O_3 chemistry for a broad variety of modelling scenarios or VOC schemes for a very restricted number of scenarios to save computing time (Liu et al., 2021; Zhong et al., 2016a). Previously, studies applied large-eddy simulation (LES) and Reynolds-averaged Navier-Stokes (RANS) models coupled with a simple NO_x-O_3 chemistry to investigate shading effects on air pollutants in street canyons (Grawe et al., 2007; Liu et al., 2021). However, the absence of VOC chemistry can introduce substantial uncertainty into model performance (Kim et al., 2012; Kwak et al., 2013), leading to sub-optimal or even mistaken strategies for air quality regulation (Dai et al., 2022).

Using a zero-dimensional, one-box, model (i.e. the well-mixed assumption for reactive species) cannot address all aspects of air quality within street canyons due to the presence of strong concentration gradients, which means that pollution "hotspots" will be undiagnosed, and too-rapid chemical dilution will occur, leading to underestimated segregation effects (Monks et al., 2015; Zhong et al., 2014). We have developed a process-based Eulerian multi-box model ("MBM-FleX") with flexible grid resolution to simulate temporal and spatial evolutions of air pollutants inside street canyons. The model uses a small number of boxes sufficient to resolve explicitly major vortices in the flow and so represent the dominant dynamical processes of advection and turbulent mixing. Compared to online LES-with-chemistry, this model design boosts computational speed very significantly and so allows computational resource to be reallocated to the investigation of broader emissions conditions and more complete VOC free-radical chemistry. MBM-FleX takes LES-derived airflow patterns in idealised regular (AR = 1) and deep (AR = 2) canyons as input, and yields a good temporal and spatial agreement with LES for a passive tracer and for reactive species (e.g. NO, NO_2, and O_3) (Dai et al., 2021). The MBM-FleX model yields comparable results regarding the spatial features of air pollutants with an extremely low computational cost for typical regular (~3 min) and deep (~6 min) canyon simulations to the LES (~10 days) (Dai et al., 2021) using a high-performance computer (HPC). Model-observation evaluations are comparable to those of other air quality models (e.g. CiTTy-Street, ADMS-urban) (Dai et al., 2022; Hood et al., 2021; Pugh et al., 2012).

Here we extended the MBM-FleX to simulate shading effects on NO_2 and O_3 inside the street canyon with different aspect ratios. It is also useful to consider the total oxidant O_x, which equals the sum of NO_2 and O_3, since these values are preserved in Carslaw and Beevers (2004). The solar-induced heating of ground and building facets induced by the solar radiation may "assist" or "oppose" air circulation, depending on the angle of solar zenith and the canyon geometry (Cai, 2012b; Paolini et al., 2014). Such thermal impacts on air flow remain highly contentious. With a temperature differential of around 10 K, previous studies indicate that the co-effects of wind-driven dynamic force due to enhanced or reduced circulation and the heating (i.e. ground and wall) alter the in-canyon flow characteristics and hence the distribution of air pollutants inside the canyons substantially (Hang et al., 2020; Liu et al., 2021; Yang et al., 2021a). Therefore, here we disentangle shading effects on atmospheric photochemistry (J values) from intricate transport-chemical interactions.

2. Experimental section

2.1. Model description

Fig. 1 presents the multi-box framework (MBM-FleX) by which the cross-sectional space of an urban street canyon has been divided into 16 and 32 boxes with an equal grid size for regular (AR = 1) and deep (AR = 2) canyons, respectively. The size and number of model boxes can vary flexibly depending on particular interests in air quality "hotspots" within canyons (Dai et al., 2021). NO_x, carbon monoxide (CO), and VOCs from anthropogenic (e.g. vehicles) and natural sources can be injected into two central boxes that represent a dual carriageway and, if necessary, into any boxes where line emissions may occur continuously. Currently, this two-dimensional (2D) MBM-FleX is settled to the case of a perpendicular background wind to the street axis because cross-canyon flow generates the most vigorous in-canyon circulations and is hence the most appropriate location to start an investigation.

Assuming the prevailing wind blows from the screen-left to the screen-right, we index the in-canyon m × n boxes using "k" for the ordinate and "i" for the abscissa directions, starting from the bottom-left (i.e. $Box_{[1,1]}$) toward top-right (i.e. $Box_{[m,n]}$). Thereby, concentrations of qth species within $Box_{[k,i]}$ and within the entire canyon are represented by $C_{q,[k,i]}$ and $C_{q,0}$, respectively. Pollutant mass exchange between neighbouring boxes within street canyons occurs through two key physical processes: advective transport, which is represented by an upwind scheme (referred to as "advective velocity"), and turbulent mixing that defined by Fick's law (referred to as "turbulent velocity"); mass exchange between canyons and the overlying background is dominated by turbulent transfer (Bright et al., 2013; Zhong et al., 2017). A linear relationship is assumed between in-canyon dynamics and prevailing wind velocities (Barlow et al., 2004; Murena et al., 2011). A flowchart (Fig. S1) in the Supporting Information is presented to describe the components of the MBM-FleX, and more information including mathematical descriptions has been detailed in a previous work (Dai et al., 2021). The code is available in both R (e.g. version 3.6.2, R Core Team (2019)) (https://github.com/ddyyqq112233/StreetX-CTM) and Fortran 90 (using the Intel Fortran (IVF) Compiler), respectively.

2.2. Model configuration

2.2.1. Street canyon geometry

Canyon geometries are taken from previous LES configurations, with the regular canyon having a street width of l_0 = 18 m and a building height of h_0 = 18 m, and with the deep canyon having l_0 = 18 m and h_0 = 36 m, respectively (Cai, 2012a; Cai, 2012b; Grawe et al., 2007). A cartesian grid used here has an x-axis that is perpendicular to the canyon and a z-axis that is vertical to the canyon. Therefore, the box resolution for both regular (4 × 4, 16 boxes) and deep (4 × 8, 32 boxes) canyons in x, z directions was Δx = 4.5 m, Δz = 4.5 m, respectively, which means that each MBM-FleX box contains 225 LES mesh elements within street canyons.

2.2.2. Airflow within canyons

Airflow field in street canyons is difficult to simulate, and it varies with factors such as building geometry, in-canyon trees, and Re number. A primary clockwise vortex and two counter-rotating vortices are observed within regular and deep canyons, respectively (Baik et al., 2007; Bright et al., 2013; Garmory et al., 2009; Zhong et al., 2017), however, a single-vortex flow regime may also be found in deep canyons

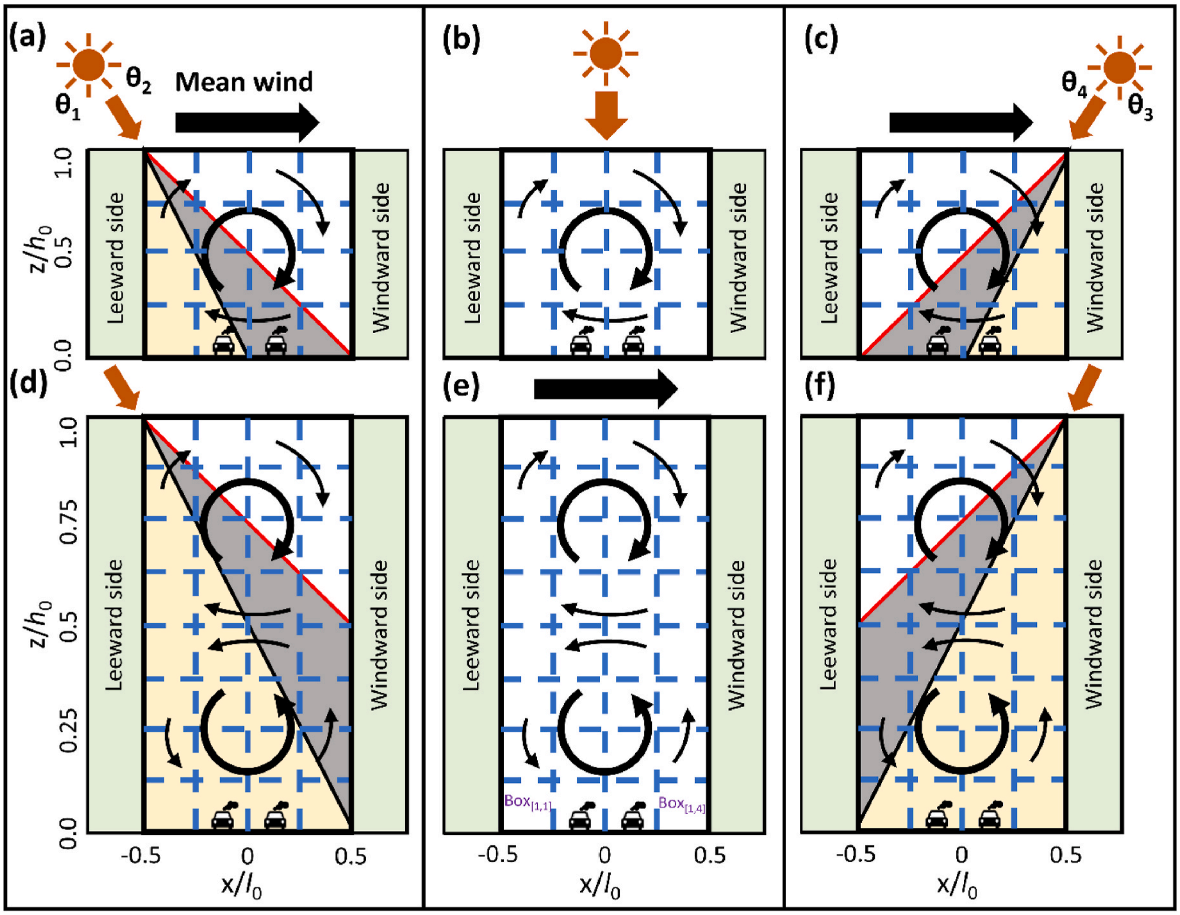

Fig. 1. The effects of sun position on regular and deep two-dimensional canyons: (a, d) leeward shading (LS) occurs when the sun is on the leeward side of canyons; (b, e) no shading (NS) when there is no shadow within canyons; (c, f) windward shading (WS) occurs when the sun is on the windward side of canyons. The canyon width $l_0 = 18$ m, and the building height $h_0 = 18$ m for the regular canyon and $h_0 = 36$ m for the deep canyon, respectively. θ_1-θ_4 represent different angles of solar zenith, resulting in half-shaded regular and deep canyons, respectively. When AR = 1 canyon is half-shaded, AR = 2 canyon is in deep shade (grey shading); when AR = 2 canyon is half-shaded, AR = 1 canyon is partially shaded (yellow shading). In-canyon vortices are also shown (curved arrows). (For interpretation of the references to colour in this figure legend, the reader is referred to the Web version of this article.)

when the independence of Re is fulfilled (Chew et al., 2018; Yang et al., 2020; Yang et al., 2021b). In this study, we applied dynamical parameters (Tables S2-S3) derived from available LES results for idealised regular and deep canyons without any in-canyon obstructions or green walls (c.f., Bright et al. (2013)), which represent flow characteristics with Re of $\sim 10^6$ at a prevailing wind speed of $U_0 = 2$ m s^{-1} in the neutral atmosphere. This also indicates the inlet boundary conditions are pre-defined, as used in the LES configuration, including a cyclic condition for the airflow in the both the *x*- and *y*-directions. The near-wall treatment (Schlichting and Kestin, 1961) was used for the flow, and a zero-flux condition was applied to all chemical species on the solid boundaries. More details and parameter derivation processes are presented in Zhong et al. (2017) and Dai et al. (2021).

2.2.3. Chemical mechanism

Two chemical schemes are applied into model simulations accounting for urban canyon chemistry, the first is a purely inorganic NO_x-O_3 chemistry that consists of reactions (1)–(3), below (Carpenter et al., 1998):

$$NO_2 + h\nu(\lambda < 410\text{nm}) \rightarrow NO + O(^3P) \tag{1}$$

$$O(^3P) + O_2 + M \rightarrow O_3 + M \tag{2}$$

$$O_3 + NO \rightarrow NO_2 + O_2 \tag{3}$$

here $h\nu$ represents the energy absorbed by the reactants where h is the Planck's constant and ν is the frequency of the absorbed light, M signifies a third-body molecule that absorbed surplus energy, reuniting O_2 and O (^{3}P) (i.e. O atoms without any excess energy that almost only are able to participate in the reaction 2) to produce an O_3 molecule. The other is a reduced chemical scheme (RCS) with 51 gas-phase species and 136 reactions derived from the Common Representative Intermediates mechanism version (CRI*v*2-R5) (Watson et al., 2008), including production of NO_2 by interaction of NO with hydroperoxyl radicals (HO_2) and peroxyl radicals (RO_2, where R is an organic molecule). Initially, model simulations were confined to midsummer daytime, and photolysis rates were derived using a two-stream isotropic scattering model at a 0.5 km altitude and a middle latitude (i.e. Birmingham, UK) under clear conditions (Table S1). Bright et al. (2013) presented full RCS details and its evaluation against CRI*v*2-R5 and the Master Chemical Mechanism (MCM*v*3) (Saunders et al., 2003).

2.2.4. Emissions

In this study, we take a busy midsummer weekday traffic scenario for a reference run (denoted as "RR") with $U_0 = 2$ m s^{-1} and 1500 on-road vehicles per hour at an average speed of 30 mph in Birmingham, UK, which is consistent with previous LES configurations (see, Bright et al. (2013); Zhong et al. (2017)); the primary NO_2: NO_x ratio (f_{NO2}) is taken as 0.1, as has been used in previous works (Bright et al., 2013; Zhong et al., 2014, 2015). The emission rates of NO_x, VOCs, and CO are 620, 127, and 1356 g km^{-1} hr^{-1}, which equate respectively to 4.44, 16, and 3.52 ppb s^{-1} for a model grid and are denoted as the "Typical Emission Scenario" (TES); VOC fractions are determined based on the annual emission mass, photochemical ozone creation potential (POCP) weighted mass and OH reactivity (Boulter et al., 2009; Bright et al., 2013), which is 44% (1.55 ppb s^{-1}) for ethene (C_2H_4), 19% (0.67 ppb s^{-1}) for propene (C_3H_6), 25% (0.88 ppb s^{-1}) for formaldehyde (HCHO), and 12% (0.42 ppb s^{-1}) for acetaldehyde (CH_3CHO); only NO_x emissions are considered for the simple NO_x-O_3 chemistry.

2.2.5. Other configurations and data processing

The initial concentrations of chemical species at $t = 0$ min (e.g. 1.3 ppb for NO, 6.78 ppb for NO_2, and 49.99 ppb for O_3) are obtained from the Tropospheric ORganic Chemistry experiment (TORCH) field campaign in suburban London (Lee et al., 2006). The multi-box models have been 'spun-up' for 30 min without any emissions to generate important atmospheric intermediates, and all chemical species at $t = 30$ min are adopted as the boundary condition (e.g. 2.5 ppb for NO, 5.6 ppb for NO_2, and 51.2 ppb for O_3) in the layer above the street canyon. Subsequently, the model is run over 210 min with emissions and chemistry, using a 0.03 s timestep, to achieve dynamical steady-state and chemical quasi-equilibrium. Data analysis is performed on simulated concentrations at $t = 240$ min.

2.3. Model scenarios

Table S4 summaries all simulated scenarios in the regular and deep canyons. Here we consider three typical scenarios for the relative direction of wind perpendicular to idealised 2D urban canyons and the sunshine throughout the daytime: (1) the leeward shading "LS" (Fig. 1a and d) indicates that street canyons beneath the top-right triangle are shaded; (2) no shading "NS" (Fig. 1b and e) indicates that no shading effects in street canyons; and (3) the windward shading "WS" (Fig. 1c and f) indicates that street canyons beneath the top-left triangle are shaded. In cases LS and WS, the angle of sun zenith is assumed to stay at 45°, θ_1 (i.e. red line in Fig. 1a and d) and θ_3 (i.e. red line in Fig. 1c and f), for regular and deep canyons, respectively, consequently the regular canyon has been half-shaded, and three quarters of the deep canyon have been shaded (see, grey plus yellow areas). A critical factor to consider in this 2D geometry is the solar zenith angle. For each shading scenario (LS and WS) for the regular and deep canyons, we adjusted the solar zenith angle respectively to 67.5°, θ_2 and θ_4, to investigate its impact on chemical processes, that is, the shaded area shrinks to the yellow area from red lines to black oblique lines. Although clouds scatter solar radiation and have daytime radiative cooling effects on urban areas (Morris et al., 2001; Nilsson and Niklasson, 1995; Weng and Fu, 2014), that is not our focus here; we assume clear conditions (i.e. cloud free, no precipitation) throughout model simulations.

The first-order rate coefficients for photochemistry (J-values) are assigned individually in each box of the MBM-FleX. For the no shading "NS" modelling scenarios, raw J-values in Table S1 are applied for RCS photochemical reactions and the value of reaction 1 is applied for the simple NO_x-O_3 chemistry in the unshaded areas, respectively. According to Finlayson-Pitts and Pitts Jr (1999), these values are scaled by 25% in the fully shaded grids and are scaled to the proportion of shading areas in the partially shaded grids, which is given by:

$$J_r = 0.25 \times J_r \times SA_f + \left(1 - SA_f\right) \times J_r = J_r\left(1 - 0.75 \times SA_f\right) \quad (4)$$

where J_r is J values for the rth photochemical reaction, SA_f is the fraction of the shaded area in the grid. Non-photochemical reaction rate coefficients are kept unchanged since the solar heating only raises air temperature by around 2–3 K (Bourbia and Awbi, 2004; Liu et al., 2021). VOC chemistry is an important contributor to the formation of NO_2 and O_3 in deep canyons (see Zhong et al. (2017)). The difference between to the two chemical schemes (i.e. reactions (1)–(3) vs. the VOC scheme) in unshaded conditions has been discussed elsewhere (Dai et al., 2022); here our focus is on how the choice of chemical scheme influences the calculated shading effects.

In this study, we also discuss the effect of shading magnitude on concentrations within street canyons. Here the original J-values in unshaded grids are multiplied by a factor of 0%, 25%, 50%, and 75% in the fully shaded grids, respectively. In order to investigate the influence of prevailing wind speed (U_0) on shading effects, J-values are held at a quarter of their original magnitudes in those fully shaded grids, while U_0 has been altered by ±40% from the RR ($U_0 = 2$ m s^{-1}) to 1.2 m s^{-1} (denoted as "LR") and 2.8 m s^{-1} (denoted as "HR"), respectively. Moreover, vehicular emissions are influenced by both traffic conditions and lane loading capability (e.g. the width of the carriageway). While maintaining $U_0 = 2$ m s^{-1} (thus, dynamical patterns within the canyon) and 25% J-values in the fully shaded grids, NO_x and VOC emission rates are normalised (i.e. $E_q/E_{q,\mathrm{TES}}$, where q refers to the qth species) by a factor of 0.05–1.0 in a step of 0.05 (i.e. 0.05, 0.10, …, 0.95, 1.0), respectively, which comprises overall 400 model simulations with different NO_x/VOC ratios.

3. Results and discussion

3.1. Effects of shading and solar zenith angles

Half of the regular canyon and three quarters of the deep canyon is shaded when the solar zenith angle is at θ_1 for LS and θ_3 for WS. In such a condition, Fig. 2 and Fig. 3 respectively present the spatial distribution of concentrations for NO_2 and O_3, and their disparities between shaded and unshaded (NS) scenarios along the leeward ($-0.5 < x/l_0 < -0.25$) and windward ($0.25 < x/l_0 < 0.5$) facades of the regular and deep canyons. The canyon averaged NO_2 and O_3 (and thus, O_x) differences alter very slightly (<1 ppb in both regular and deep canyons) as the solar zenith angle moves from LS (solid lines) to WS (dashed lines), which suggests little difference in pollution mass transfer from street canyons to the upper background when the solar zenith angle is such that the regular canyon is half-shaded. However, LS and WS obviously affect the spatial distribution of pollutants within street canyons. Following the course of the primary vortex in the regular canyon (Fig. 2), NO_2 and O_3 differences due to the shading grow more pronounced when the air passes through the shaded area, but soon lessen quickly as the air reaches the unshaded area. Therefore, LS has a greater influence on ground concentrations on the leeward side ($\mathrm{Box}_{[1,1]}$), while WS has a greater influence on the windward side ($\mathrm{Box}_{[1,4]}$). Moreover, shifting from the LS to WS in the regular canyon, the ground NO_2 differences with respect to the unshaded run range from 5.0 ppb (5.3%) to 2.8 ppb (2.9%) on the leeward side and from 1.2 ppb (1.9%) to 6.1 ppb (9.5%) on the windward side; while the ground O_3 difference decreases range from −7.5 ppb (−67.4%) to −5.1 ppb (−46.0%) on the leeward side and from −2.8 ppb (−22.2%) to −7.7 ppb (−61.2%) on the windward side, respectively. With the air moving toward the unshaded area near the rooftop, concentration differences are smaller than those at the pedestrian level due to the enhanced photodissociation, which is consistent with LES modelling (c.f., Grawe et al. (2007)).

In the deep canyon (Fig. 3), the upper vortex is formed by the turbulent effect induced by wind shear near the building rooftop (Zhong et al., 2015), just as for the regular canyon, resulting in similar (but more pronounced) NO_2 and O_3 patterns under the different shading scenarios. For the LS, NO_2 and O_3 concentration differences are up to 7.2 ppb (5.4%) and −9.7 ppb (−67.4%) in $\mathrm{Box}_{[1,6]}$ on the leeward side. For the WS, the differences are up to 8.5 ppb (7.9%) and −10.4 ppb (−63.3%) in $\mathrm{Box}_{[4,6]}$ on the windward side, respectively. The differences decline rapidly in the lower compartment, within which a minor counter-clockwise vortex is generated by wind shear at the middle of the canyon, and the shading effects become less important as the lower compartment has been fully shaded under both LS and WS. NO_2 decreases somewhat (<2 ppb) as a result of reduced contributions from VOC chemistry; that

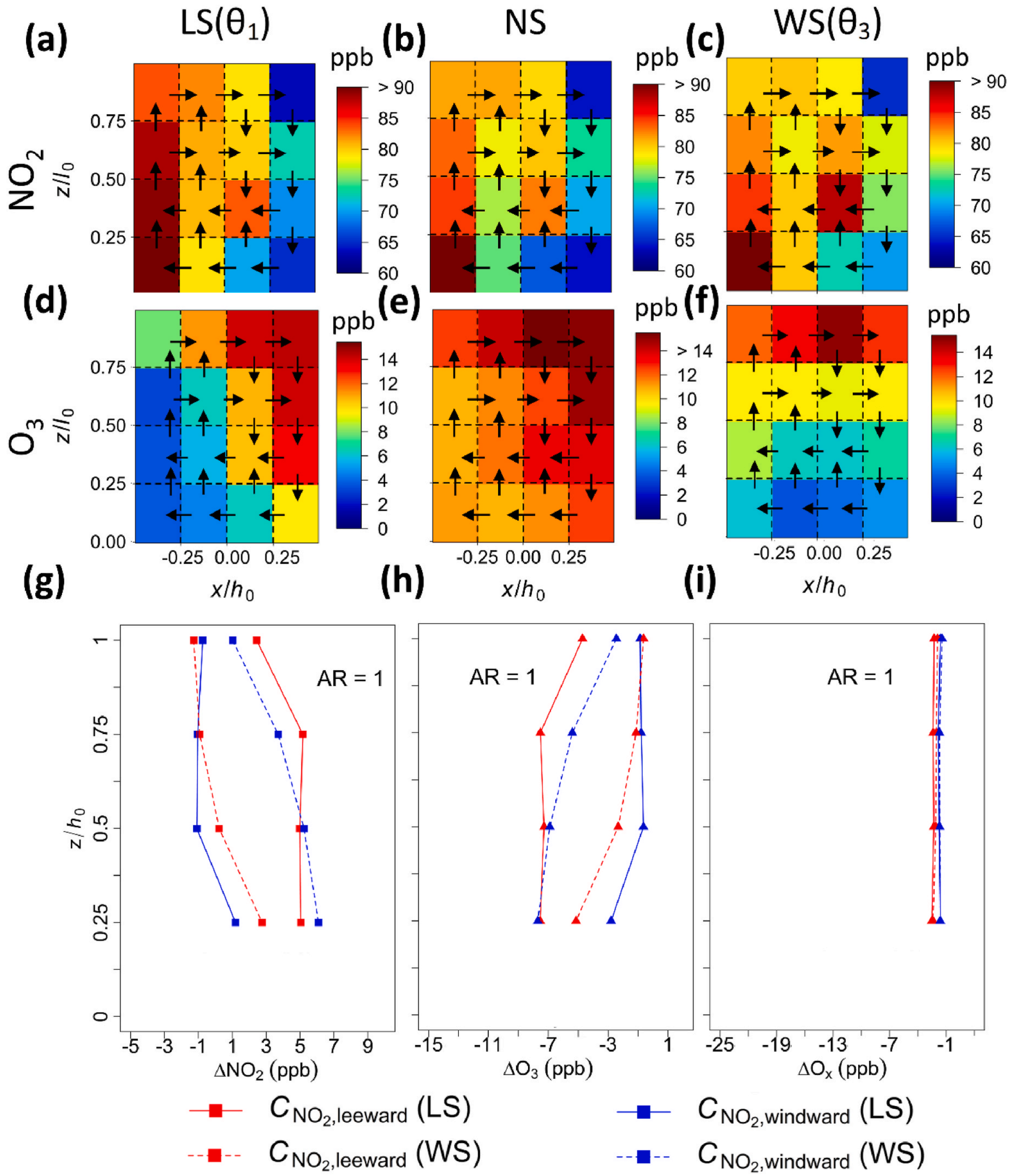

Fig. 2. The spatial distribution of NO_2 and O_3 (ppb) under lee-side (θ_1) and wind-side (θ_3) shading with a quarter of original *J*-values of RCS chemistry in the regular canyon (first and second rows). Line graph panels g–i present concentration differences with respect to a no-shading simulation (values of shaded situations LS and WS subtracted from those of the unshaded scenarios NS) for NO_2, O_3, and O_x in the regular canyons, respectively. The solar zenith angle is such that the regular canyon is half-shaded. Subscripts "leeward" and "windward" represent the magnitude of differences along with the leeward wall ($-0.5 < x/l_0 < -0.25$) and the windward wall ($0.25 < x/l_0 < 0.5$), respectively. Arrows give an illustration of the advective flow in the canyon. See text for details.

is, the production of HO_2 and RO_2 has been constrained under the shading scenarios. O_3 levels at the lower compartment stay rather stable due to intricate transport-chemical processes. The concentration of O_x decreases slightly (<2 ppb) because of the formation of nitric acid (HNO_3) insides deep canyons.

Considering the solar zenith angle at which the deep canyon is half-shaded (θ_2 and θ_4), Fig. 4 shows the spatial distribution of concentration differences for NO_2, O_3, and O_x within the regular canyon along the leeward and windward facades. In comparison to the "half-shaded regular canyon" scenario (Fig. 2), the spatial distribution of pollutant differences is similar, although ground NO_2 and O_3 differences are somewhat decreased under varying shading conditions. When full sunlight crosses through both the upper clockwise and lower anti-clockwise vortices of the deep canyon (Fig. 5), NO_2 and O_3 reduce substantially under the shading scenarios, leading to larger concentration differences. From LS (θ_2) to WS (θ_4), ground NO_2 differences slightly increase from −1.4 ppb (−0.9%) to −3.2 ppb (−2.0%) on the leeward side and from −13.8 ppb (−5.2%) to −16.1 ppb (−6.1%) on the windward side. Ground O_3 differences change from −11.0 ppb (−75.4%) to −8.1 ppb (−55.6%) on the leeward side and from −5.0 ppb (−59.5%) to −6.4 ppb

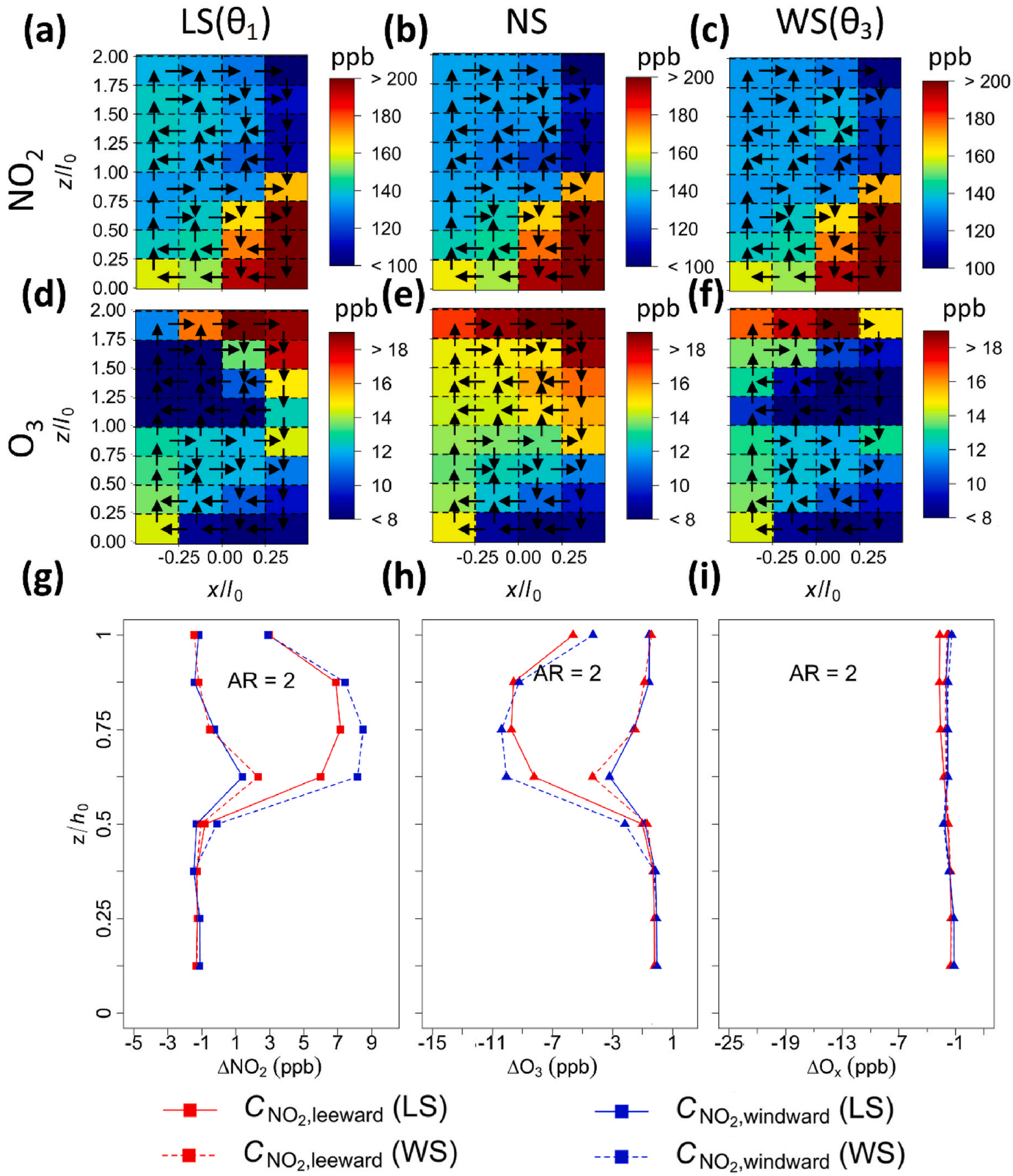

Fig. 3. The spatial distribution of NO_2 and O_3 (ppb) under lee-side (θ_1) and wind-side (θ_3) shading with a quarter of original *J*-values of RCS chemistry in the deep canyon. Line graph panels g–i present concentration differences with respect to a no-shading simulation (values of shaded situations LS and WS subtracted from those of the unshaded scenarios NS) for NO_2, O_3, and O_x in the deep canyon. The solar zenith angle is such that the regular canyon is half-shaded. Subscripts "leeward" and "windward" represent the magnitude of differences along with the leeward wall ($-0.5 < x/l_0 < -0.25$) and the windward wall ($0.25 < x/l_0 < 0.5$), respectively. Arrows give an illustration of the advective flow in the canyon. See text for details.

(−77.1%) on the windward side, respectively.

Our results show that shading effects modify the spatial distribution of reactive species within street canyons depending on the canyon geometry and solar zenith angle. Interestingly, although NO_2 photodegradation rate has been reduced from 9.20×10^{-3} s^{-1} to 2.30×10^{-3} s^{-1} when the deep canyon is half-shaded, NO_2 concentrations within the deep canyon become lower by up to ~9% because of the shade. Also, O_x is a useful measure of the street canyon chemistry and its difference due to the shade decreases slightly in the regular canyon but decreases substantially up to 23 ppb (~7%) inside the deep canyon, which can be attributed to the inclusion of VOC chemistry as it becomes more important when air residence times are longer. This is further discussed in the following section by model simulations using the simple NO_x-O_3 chemistry.

3.2. Effects of VOC chemistry

Inclusion of VOCs emissions from on-road vehicles can affect photochemical reactions, especially in deep urban canyons with longer residence times of air pollutants (Zhong et al., 2017). CFD-based models,

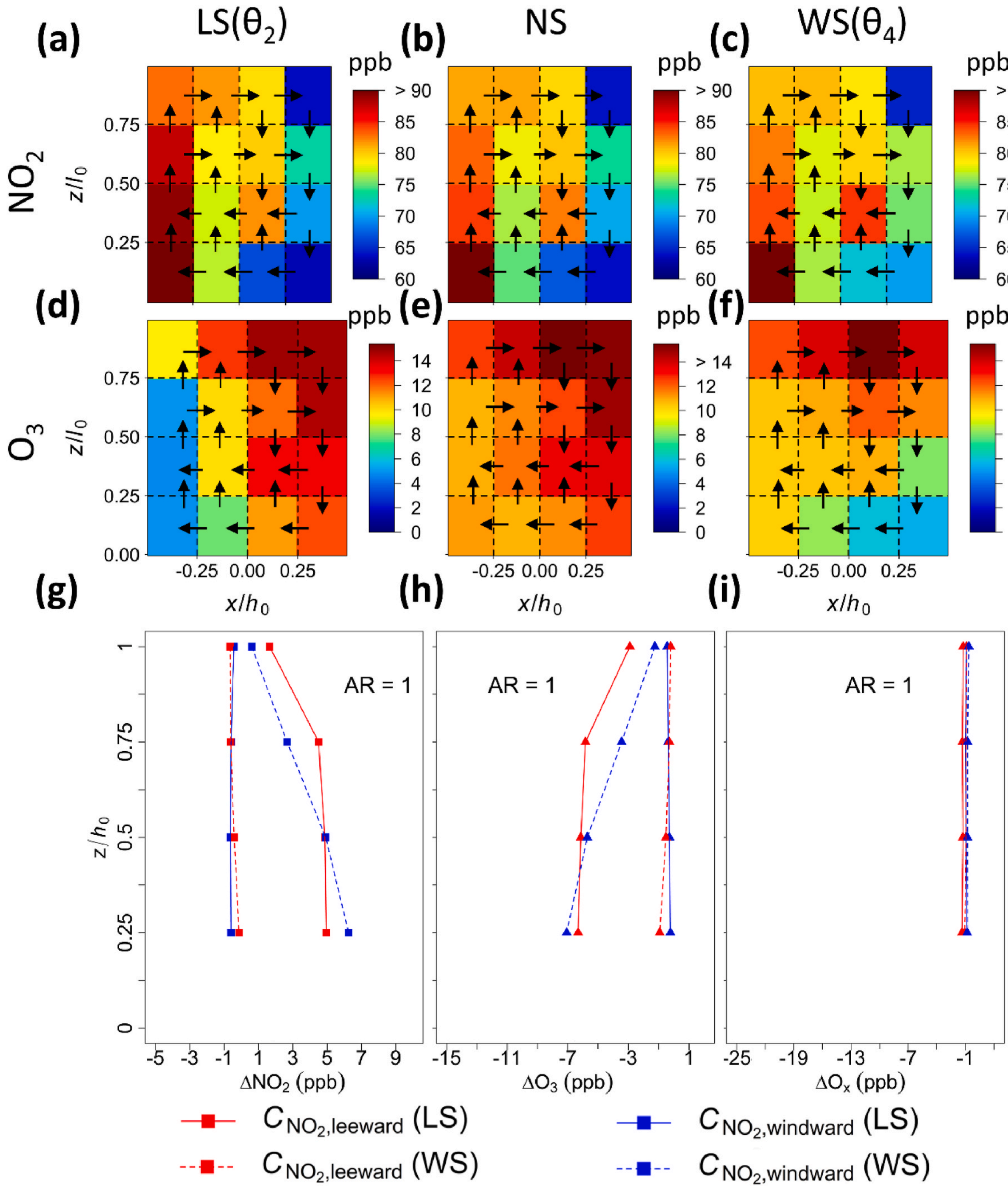

Fig. 4. The spatial distribution of NO_2 and O_3 (ppb) under lee-side (θ_2) and wind-side (θ_4) shading with a quarter of original *J*-values of RCS chemistry in the regular canyon. Line graph panels a–c present concentration differences with respect to a no-shading simulation (values of shaded situations LS and WS subtracted from those of the unshaded scenarios NS) for NO_2, O_3, and O_x in the regular canyons, respectively. The solar zenith angle is such that the deep canyon is half-shaded (θ_2 and θ_4). Subscripts "leeward" and "windward" represent the magnitude of differences along with the leeward wall ($-0.5 < x/l_0 < -0.25$) and windward wall ($0.25 < x/l_0 < 0.5$), respectively. Arrows give an illustration of the advective flow in the canyon. See text for details.

in general, simulate air quality within street canyons or across densely built regions coupled only to a simple NO_x-O_3 cycle to conserve computational resources. Shading affects not only NO_2 photolysis, but also several VOC free-radical reactions (e.g. Table S1). Using simple NO_x-O_3 chemistry at different solar zenith angles, Fig. 6 gives the spatial distribution of concentration differences between the shaded scenarios and the unshaded scenario for NO_2, O_3, and O_x in regular and deep canyons. Fig. S3 provides the percentage underestimation of NO_2, O_3, and O_x concentrations spatially within street canyons due to shading effects (see Figs. S3–S6 for the spatial distribution of absolute values).

Considering the shading scenarios, the loss of photon flux causes NO_2 to rise regardless of the solar zenith angle, which can also be observed when VOC chemistry is negligible (e.g. see Figs. 2a and 3a for NO_2 distributions in the regular canyon). When only the simple chemistry is considered, O_x can be regarded as a passive tracer, since changes in NO_2 are compensated by opposite changes in O_3. O_x concentrations are always conserved between the shaded scenarios and the unshaded scenario (Fig. 6c, f, 6i, 6 l). Therefore, the magnitudes of O_3 depletion are similar to that of increased NO_2 but opposite in sign (e.g., positive NO_2 and negative O_3 differences accordingly of 5 ppb along the leeward wall

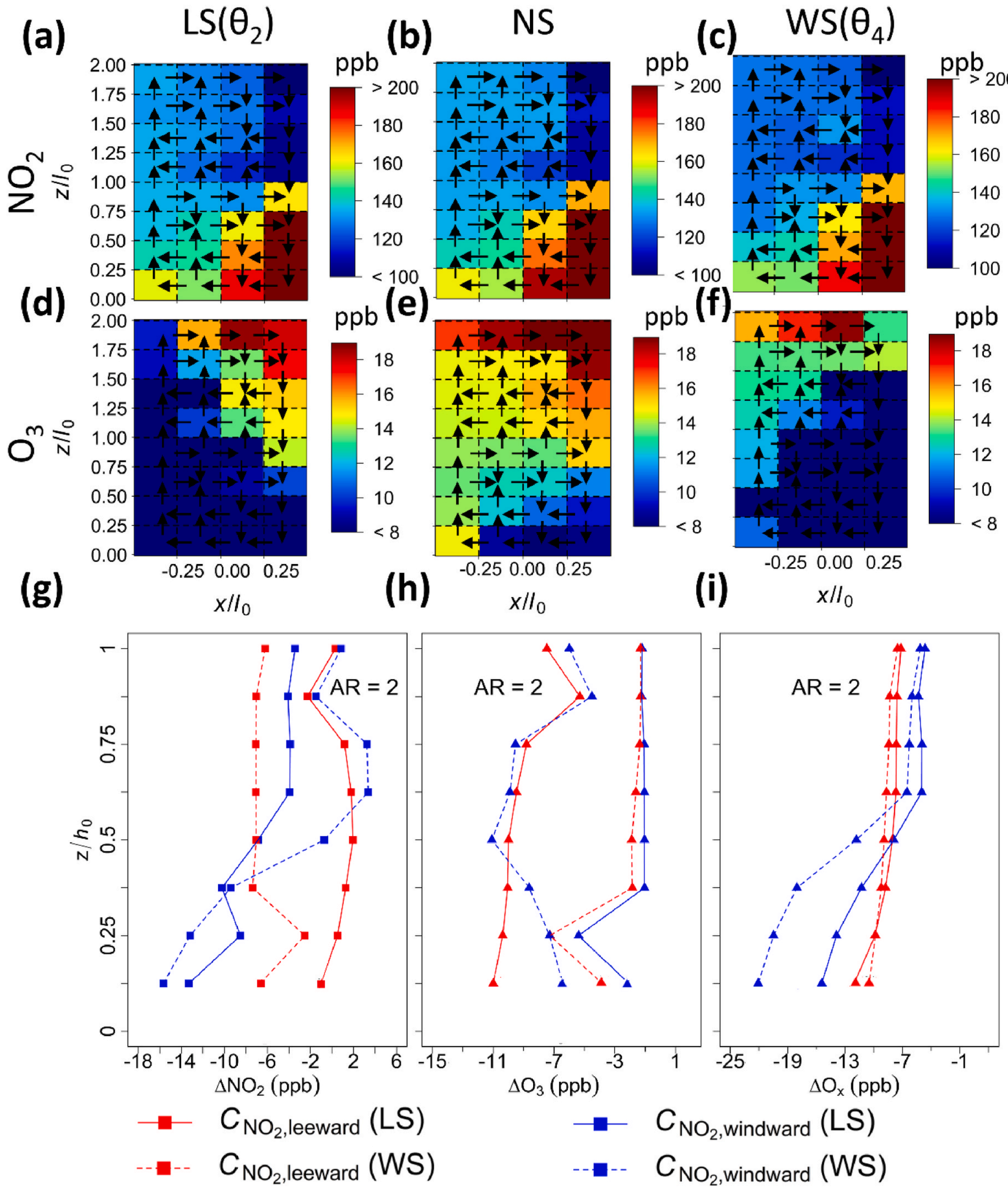

Fig. 5. The spatial distribution of NO_2 and O_3 (ppb) under lee-side (θ_2) and wind-side (θ_4) shading with a quarter of original *J*-values of RCS chemistry in the deep canyon. Line graph panels g–i present concentration differences with respect to a no-shading simulation (values of shaded situations LS and WS subtracted from those of the unshaded scenarios NS) for NO_2, O_3, and O_x in the regular canyons, respectively. The solar zenith angle is such that the deep canyon is half-shaded (θ_2 and θ_4). Subscripts "leeward" and "windward" represent the magnitude of differences along with the leeward wall ($-0.5 < x/l_0 < -0.25$) and windward wall ($0.25 < x/l_0 < 0.5$), respectively. Arrows give an illustration of the advective flow in the canyon. See text for details.

under the LS) (Grawe et al., 2007). Although the spatial distribution of concentration differences between shading and unshaded scenarios still varies with solar zenith angle, these changes in concentration are less important for NO_2 (up to ~10%) but remain substantial for O_3 (up to ~75%).

Our results indicate not only that simulations using the RCS scheme capture O_3 production or depletion more precisely (Muilwijk et al., 2016), but also the importance of shading effects on NO_2. Reduced photolysis rates constrain the generation of hydroperoxyl radicals (HO_2), thus limiting the synthesis of NO_2 through the oxidation of NO. NO_2 concentrations decrease by 0.1%–7% due to the shading effects when VOC chemistry becomes important (see, Fig. 5g). Therefore, the RCS model describes the proper mechanics of O_x depletion as a function of the local availability of VOC free radicals and the solar energy, which cannot be simulated by using the simple NO_x-O_3 cycle.

Absolute values of NO_2 and O_3 can be considerably underestimated without considering VOC chemistry. For example, the averaged NO_2 increases from 85 ppb to 136 ppb (37%) and O_3 from 7 ppb to 13 ppb (46%) in the idealised deep canyon (Zhong et al., 2017). One might ask whether these disparities, caused by different chemical schemes, can be

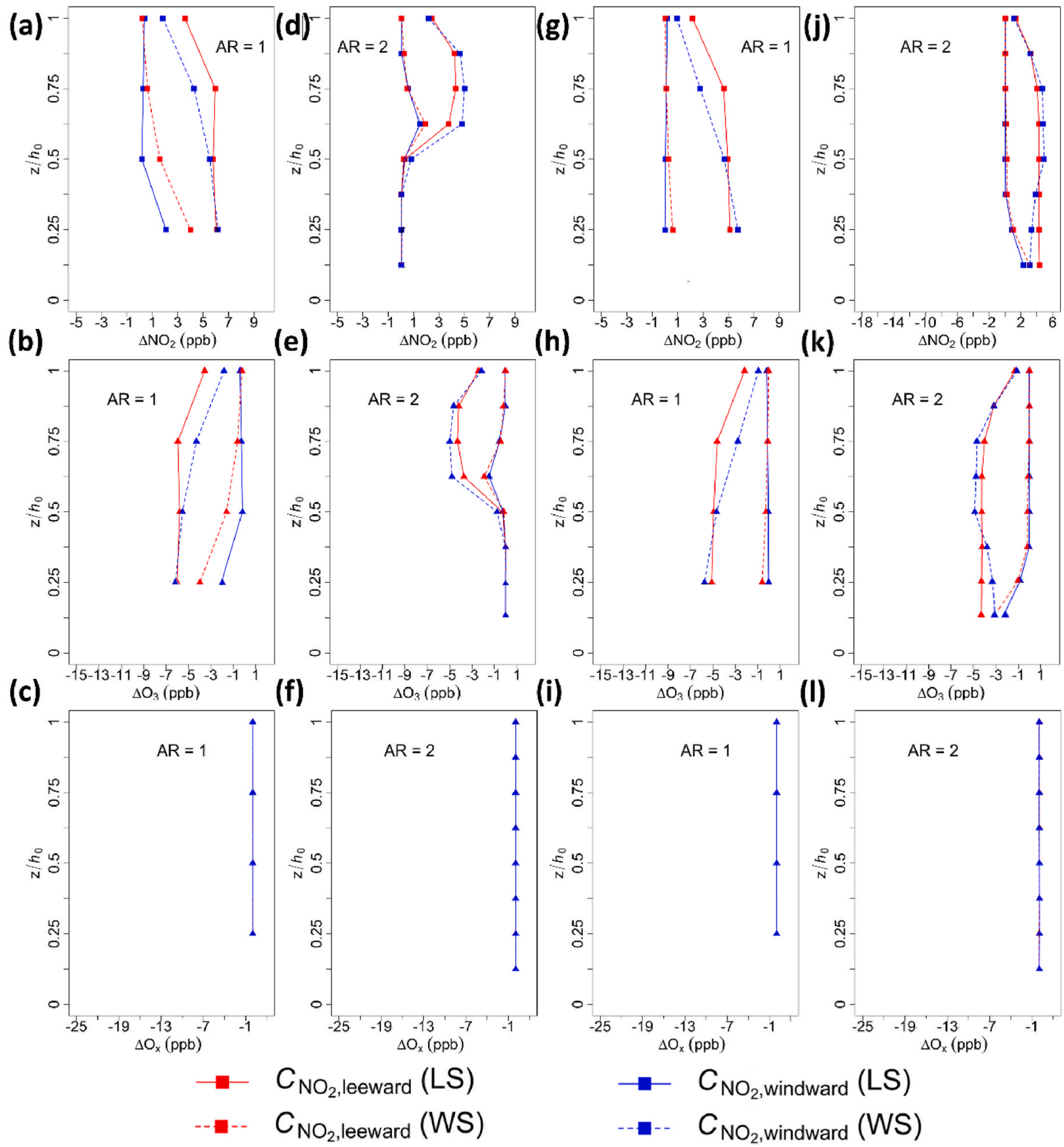

Fig. 6. The spatial distribution of concentration differences for NO_2, O_3, and O_x in ppb by using the **simple NO_x-O_3 chemistry** in regular (a, b, c, g, h, i) and deep (d, e, f, j, k, l) street canyons. All differences are with respect to a no-shading simulation. The solar zenith angle is such that the regular canyon is half-shaded (θ_1 and θ_3) for figures a–f; and the angle is such that the deep canyon is half-shaded (θ_2 and θ_4) for figures g–l. Subscripts "lee" and "wind" represent the magnitude of differences along with the leeward wall ($-0.5 < x/l_0 < -0.25$) and windward wall ($0.25 < x/l_0 < 0.5$), respectively.

offset by shading effects. Without shading (i.e. NS), underestimates of NO_2 by using the simple NO_x-O_3 cycle are ~13% and ~41% in the regular and deep canyons compared to those of using VOC chemistry; and underestimates of O_3 are ~20% and ~55%, respectively (Fig. 5). Considering the effect of including shading on the underestimates of simple chemistry, the magnitude of the underestimate varies with solar zenith angle and canyon geometry. When the regular canyon has been half-shaded, O_3 underestimates change remarkably to ~35% and ~22% in regular and deep canyons, respectively; when the deep canyon has been half-shaded, the canyon averaged underestimations are similar to those of NS in the regular canyon but decrease to ~37% for NO_2 and to ~31% for O_3 in the deep canyon, respectively. It is worth noting that the underestimate of O_3 varies spatially within street canyons (e.g. ~50% at the pedestrian level and ~15% at the rooftop of the deep canyon). There is no single and simple factor that can be used to bridge the gap between concentration differences due to different chemical schemes, with or without shading, which emphasizes the need to include shading effects along with VOC free-radical chemistry in future air quality simulations.

3.3. Effects of NO_x and VOC emissions

The response of atmospheric chemistry to anthropogenic emissions is complex and highly non-linear (Colbeck and MacKenzie, 1994; Seinfeld and Pandis, 2008). It is therefore likely that shading effects will vary with on-road conditions such as vehicle types and emission factors. While greater percentage uncertainties in O_3 concentrations are found under a typical traffic condition (as discussed above), their absolute values are not significant. Nonetheless, shifting traffic emissions also alter the chemistry in the urban environment, potentially yielding more O_3 to the critical level higher than 40 ppb and causing adverse effects on public health and plants (Bortier et al., 2000; Satsangi et al., 2004). Therefore, we examined various emission conditions to investigate their impacts on shading effects. Here we adopt percentage differences to assess shading effects on NO_2 and O_3 levels within urban canyons because varying traffic emissions lead to different absolute values of air pollution. Results are illustrated in Fig. 7 and Fig. 8 using isopleths similar to those used in O_3-NO_x-VOC sensitivity studies (Sillman, 1999).

Fig. 7 shows that NO_x and VOC emissions have considerable impact on shading effects in a non-linear fashion when the solar zenith angle is such that the regular canyon is half-shaded, but the pattern changes little with the shading scenarios (i.e. LS and WS). Lower traffic emissions lead to stronger relative changes due to shading on NO_2 by up to ~10% and ~5% in regular and deep canyons, respectively, but result in weaker shading effects on O_3 by up to ~23% and ~13%, respectively. The shading effects on NO_2 are more sensitive to NO_x than they are to VOC emissions, particularly under a high-NO_x circumstance within street canyons, but shading becomes more susceptible to VOCs when NO_x emissions are low. The shading effects on O_3 change very slightly with VOC emissions but increase greatly with increasing NO_x emissions. When the solar zenith angle is such that the deep canyon is half-shaded and the regular canyon is less shaded (Fig. 1), the sensitivity of shading effects to emissions decreases in the regular canyon (e.g. varying <2% for in-canyon NO_2; Fig. 8) but significantly increases in the deep canyon. In the NO_x-sensitive (or VOC-saturated) zone, the shading effect increases with increasing NO_x emissions and shows relatively little change in response to increased VOC emissions.

The solid line in each panel of Figs. 7 and 8 depicts emission conditions leading to the critical level of NO_2 (105 ppb) and O_3 (40 ppb) without shading, whereas the dashed line gives the critical-level emission conditions with shading. The disparity between the lines indicates that model simulations without shading provide imprecise determination of compliance, particularly for O_3 concentrations within the urban canyon environment. Despite that results indicate that neglecting shade has a little effect on compliance with the air quality threshold for the canyon-average value, it should be noted that half-shading situations with very high VOC:NO_x ratios might be significant if internal combustion vehicles are phased out, removing NO_x but leaving VOC emissions from solvent evaporation and biogenic VOCs, which could be discussed further. Model results for the regular canyon in our work vary from those of a prior work (Grawe et al., 2007) because to the existence of VOC free-radical interactions that violate O_x conservation, which suggests the shading effects and VOC free-radical chemical reactions need to be considered properly particularly for the deep canyon modelling.

3.4. Effects of shading intensities

Fig. 9 and Fig. S7 provide the concentration difference for NO_2 and O_3 between the shaded scenarios (LS and WS) and NS under different chemical schemes with the photolysis rate of various percentages of their original values in shaded grids of street canyons. In the regular canyon, as with Grawe et al. (2007), the shade overall causes increased canyon averaged NO_2 and decreased O_3 (i.e. $C_{NO2,0}$ and $C_{O3,0}$, denoted by black lines in our figures) due to reduced efficiencies of NO_2 photolysis (reaction (1), above) and, hence, reduced O_3 formation (Fig. 9a and c, S6a, S6c). There is a nearly linear relationship between concentration differences and the shading magnitude, as those in Grawe et al. (2007), for all shading scenarios and locations shown except NO_2 in the deep-canyon, half-shading scenario (Fig. 9b). In the deep canyon, where chemistry has more time to take place, the relationship between the shading magnitude and NO_2 differences depends on both the solar zenith angle and chemical schemes. Fig. 9d and Fig. S7d indicate that the efficiency of NO_2 dissociation alone cannot be responsible for non-linear effects. With VOC free-radical chemistry, a near linear relationship between NO_2 and O_3 concentration differences and the shading magnitude is found when the regular canyon has been half-shaded (i.e. the solar

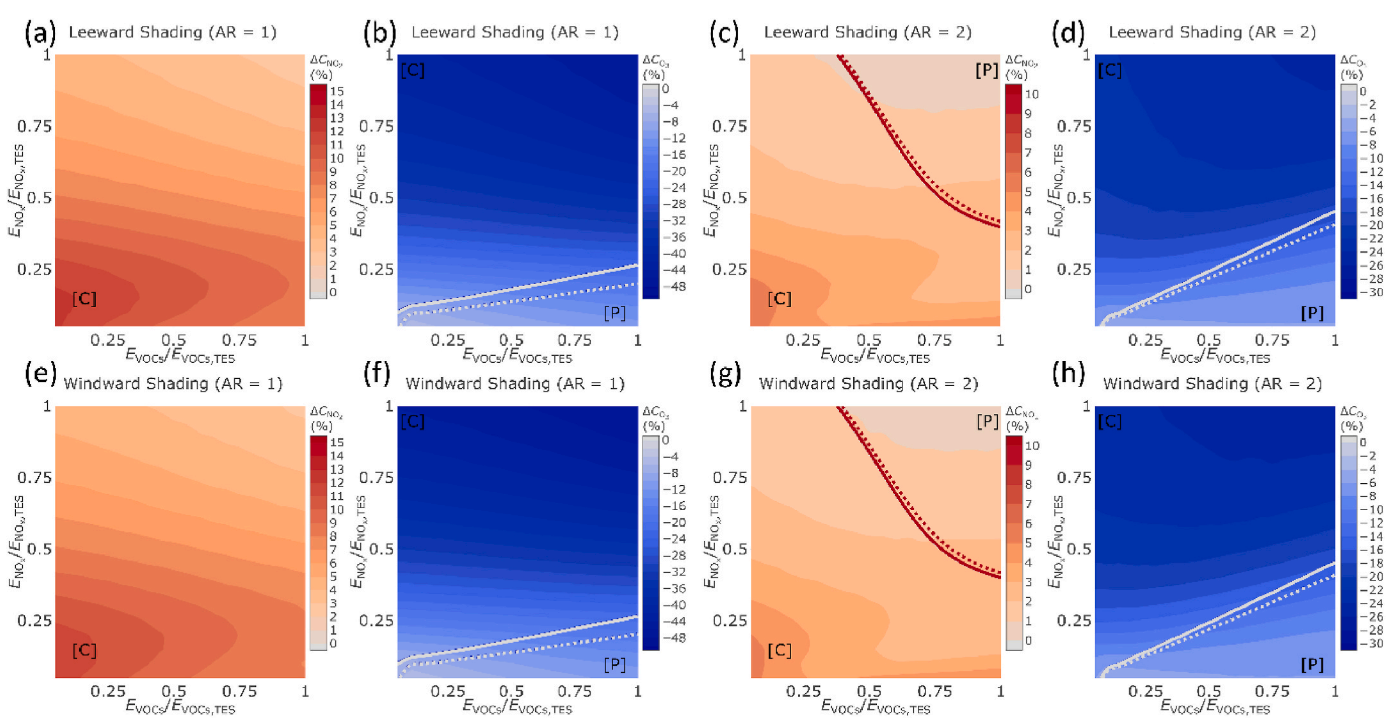

Fig. 7. The percentage difference (%) in canyon-averaged NO_2 and O_3 due to the shading effects (one quarter of original *J*-values in fully shaded grids) for RCS chemistry in regular and deep canyons at different NO_x and VOC emission rates. The solar zenith angle is such that the regular canyon is half-shaded (θ_1 and θ_3). The solid contour represents the critical level of NO_2 (105 ppb) and O_3 (40 ppb) under the unshaded scenario, and the dash contour represents the critical level under the shaded scenario. The Region "[P]" represents the polluted air zone where air pollution concentrations exceed the objective, and the Region "[C]" represents the clear air zone where the air quality is in compliance with the objective.

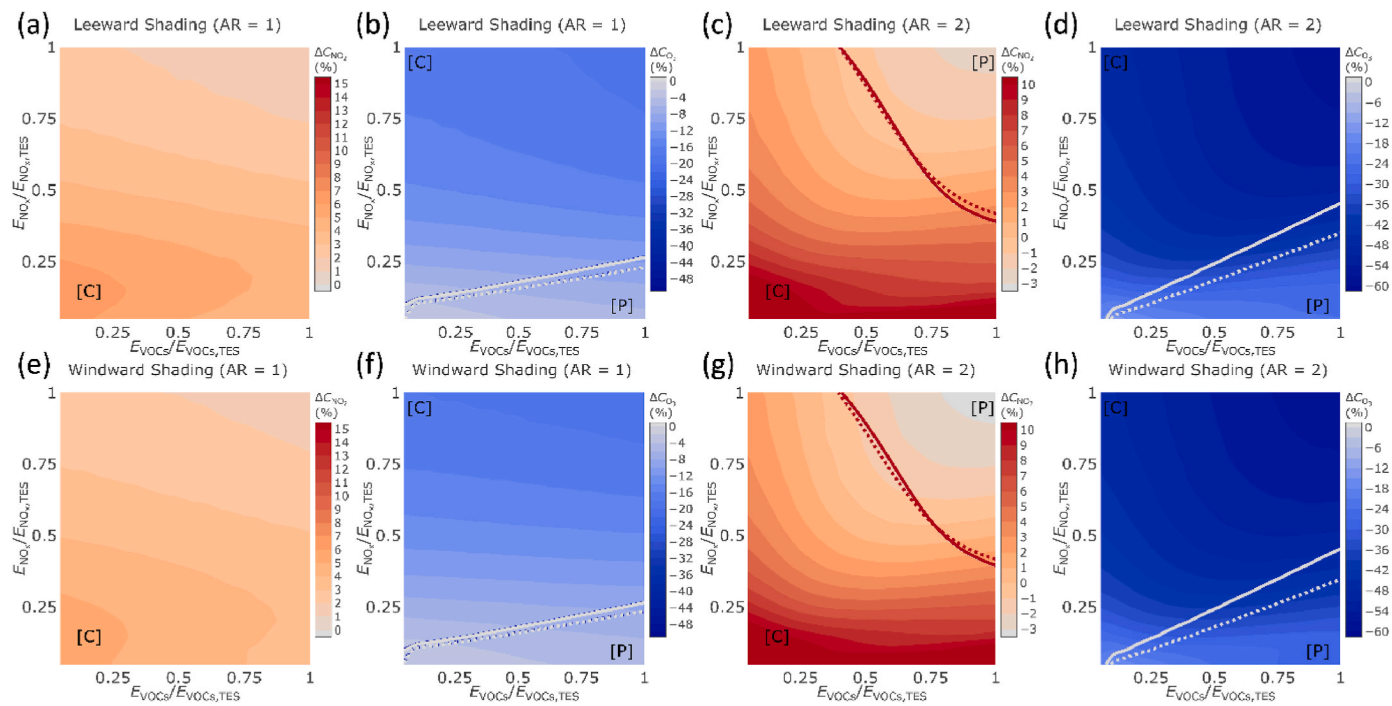

Fig. 8. The percentage difference (%) in canyon-averaged NO_2 and O_3 due to the shading effects (one quarter of original *J*-values in fully shaded grids) for RCS chemistry in regular and deep canyons at different NO_x and VOC emission rates. The solar zenith angle is such that the deep canyon is half-shaded (θ_2 and θ_4). The solid contour represents the critical level of NO_2 (105 ppb) and O_3 (40 ppb) under the unshaded scenario, and the dash contour represents the critical level under the shaded scenario. The Region "[P]" represents the polluted air zone where air pollution concentrations exceed the objective, and the Region "[C]" represents the clear air zone where the air quality is in compliance with the objective.

zenith angle is θ_1 or θ_3, Fig. S7b). However, when the deep canyon is half-shaded (i.e. the solar zenith angle is θ_2 or θ_4), the linear hypothesis between concentrations and the shading magnitude is still valid for O_3 but is not valid for NO_2, because NO_2 differences increase non-linearly with the photolysis efficiency and vary very little throughout a range of shading magnitudes on the lee-side façade in the deep canyon. Therefore, using the simple NO_x-O_3 chemistry can lead to erroneous estimates of air quality and subsequent health impacts, as the simple linear assumption between NO_2 and shade intensity is no longer applicable when VOC free-radical chemistry is involved. This is particularly important for urban networks in middle latitudes with a high density of tall buildings because of sufficient shade and poor ventilation, which highlights the necessity of considering VOC reactions for physico-chemical process simulations in the real atmosphere.

3.5. *Effects of prevailing wind speeds*

The prevailing wind speed (U_0) affects the mass exchange efficiency between the street canyon and the overlying background, leading to changes in resident time of chemical species and in the distribution of pollutant concentrations within street canyons (Murena et al., 2011). Higher U_0 (e.g. 2.8 m s^{-1}) enables not only enhanced rooftop ventilation but also more rapid in-canyon air circulation between shaded and unshaded areas inside the urban canyon (Grawe et al., 2007), while lower U_0 (e.g. 1.2 m s^{-1}) allows chemistry to occur for longer time (Park et al., 2015). Albeit that using scaled dynamical parameters cannot describe in-canyon airflow characteristics absolutely accurately, the objective here is to investigate in broad terms the impact of canyon ventilation on the shading effects associated with solar zenith angle and canyon geometry. When the regular canyon is half-shaded, absolute shading-non-shading differences for NO_2 and O_3 are small (as shown in Fig. S8). Increased U_0 leads to markedly lower NO_2 and higher O_3 inside street canyons due to a stronger mixing between the canyon and the background (Zhong et al., 2016b). Therefore, considering the percent variance, in the regular canyon, NO_2 reduces somewhat (to ~1%) as a result of shading effects due to decreased efficiency of formation through VOC chemistry at lower U_0, while NO_2 concentrations rise by 5% at higher U_0, because of VOC chemistry. Differences in O_3 decrease from ~38% to ~29% with increasing wind speeds. In the deep canyon, the impact of changes in prevailing wind velocity on the shading effects is quite small (<2%) for NO_2 and O_3 due to its impacts on both physical and chemical processes. When the deep canyon is half-shaded (Fig. S9), the pattern of concentration changes inside the regular canyon is very similar to that of the "half-shaded regular canyon" condition (i.e. from −1% to 2% for NO_2 and from −20% to −15% for O_3). The differences drop substantially with increased U_0 in particular for ground NO_2 on the windward side (e.g. from −38 ppb and −32 ppb to −8 ppb for WS and LS, respectively), however, these changes in percentage are small (from ~-8% to ~ -4%), because ground NO_2 concentrations can be extremely high (e.g. up to ~230 ppb) in the deep canyon at low U_0 (Murena et al., 2009; Zhong et al., 2015). The shading effects on the canyon average O_3 decrease slightly (<3%) as U_0 increases, but larger wind impacts are observed at different locations inside the canyon (e.g. ~15% along the windward side). Consequently, the impact of prevailing wind speed on shading effects cannot be disregarded because location-specific concentrations need to be predicted accurately in order to develop targeted and effective strategies.

In this study, MBM-FleX provides a method for coupling different chemical schemes to simulate reactive species in urban canyons. Inevitably, the current model has some limitations. Firstly, the dynamical parameters (advective velocity and turbulent velocity) need to be derived from a pre-computed RANS or LES model; in other words, the airflow characteristics are predefined in MBM-FleX. Secondly, while the resolution of the model is adjustable, a higher resolution leads to better capture of segregation effects (Li et al., 2021; Zhong et al., 2014) but an exponentially increasing number of dynamical parameters. There is always a trade-off between the number of meshes and the computation time. Thirdly, MBM-FleX is only applicable when the predominant wind

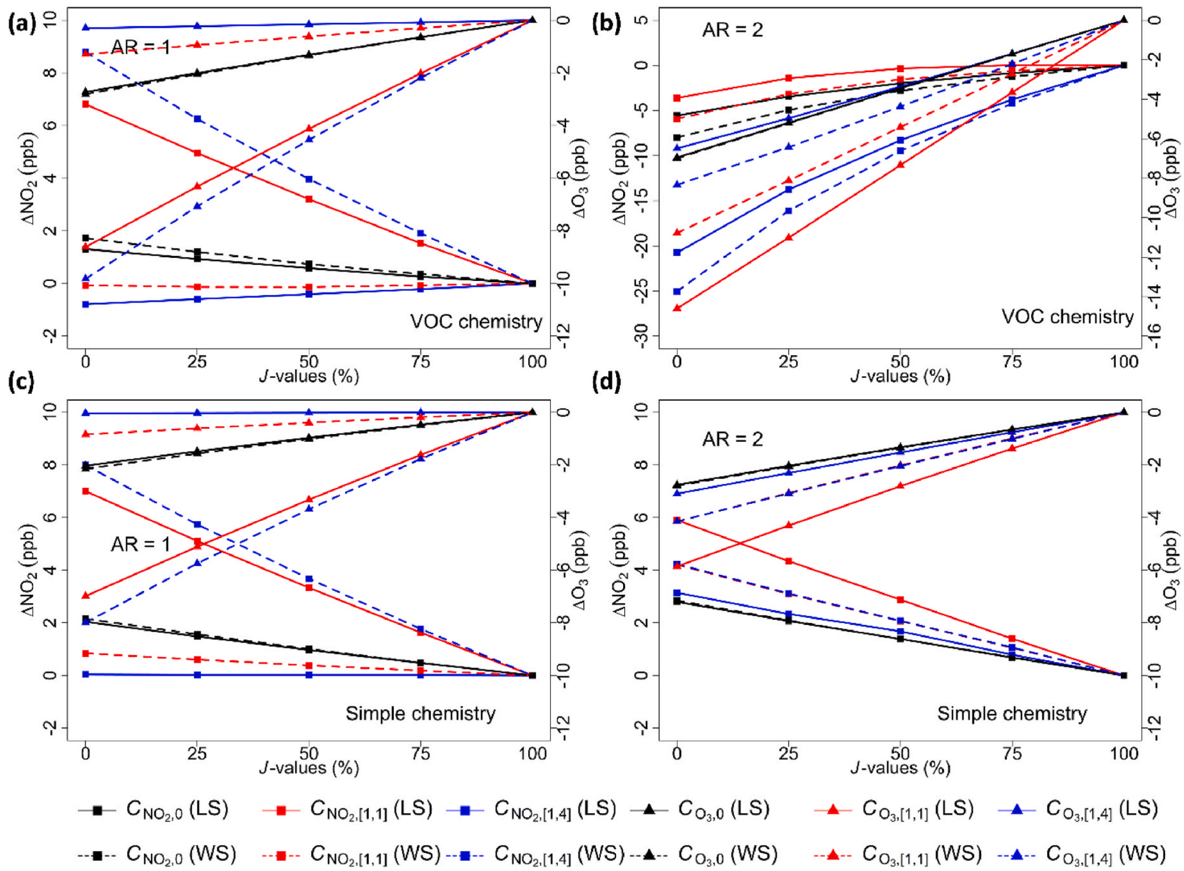

Fig. 9. Concentration differences in NO_2 and O_3 (ppb) under different photolysis rates in RCS and simple NO_x-O_3 chemistry that denoted by percentages of their original values in regular and deep canyons, respectively. The sun zenith angle is such that the deep canyon is half-shaded and the regular canyon lightly shaded (θ_2 and θ_4). Line colours indicate different locations of street canyons (the entire canyon and the pavement); line types indicate concentrations of different shading scenarios (LS and WS) minus those of NS; and squares and triangles represent NO_2 and O_3, respectively. Note the change of y-axis scales between top-right and bottom-right panels. (For interpretation of the references to colour in this figure legend, the reader is referred to the Web version of this article.)

direction is perpendicular to the street axis. In light of these complications, more studies into the shading effects on air quality at street-to-regional scale is necessary to improve the rationale of urban design.

4. Conclusions

The poorly ventilated nature of urban canyons leads to frequent occurrences of severe air pollution, affecting the health of pedestrians who are exposed in such environments. Therefore, urban canyons become “hotspots” areas for air quality management. A processed-based multi-box model (MBM-FleX) coupled with chemical schemes was implemented to investigate shading effects on NO_2, O_3, and O_x (NO_2 + O_3) within urban street canyons. Our results reveal sometimes large differences between the shaded and unshaded scenarios, demonstrating that the interaction of shading effects, chemical processes, emissions, and tracer transport alter the average magnitude and spatial distribution of air pollution within street canyons. When the solar zenith angle is such that a regular canyon (aspect ratio ≈ 1) is half-shaded, NO_2 and O_3 differences caused by the shading effects become more significant as air blows through the shaded areas, but quickly reduced when the air moves into the unshaded areas due to enhanced photochemistry. In the deep street canyon, considering the same angle of incident sunlight, the concentration differences rapidly lessen and the shading effects become less significant in the lower compartment as it is completely shaded on both lee- and wind-side directions. The spatial distribution of pollutants in the regular canyon overall are similar when solar zenith angle changes in this study, while concentration differences within the deep canyon increase significantly.

With the simple NO_x-O_3 chemistry, shade slows the photodegradation of NO_2, causing NO_2 concentrations to increase inside street canyons, while O_3 concentrations always vary in an opposite manner due to O_x conservation. Our results reveal that VOC chemistry can be of importance in modelling shading effects in terms of its impact on, in particular, O_x concentrations in street canyons, which becomes crucial when the generation of NO_2 from the oxidation of NO with hydroperoxyl radical (HO_2) is substantial. Additionally, the difference in O_3 between shaded and unshaded scenarios is linearly related to shading intensity, but the shaded-unshaded difference in NO_2 is not linearly related to shading intensity, especially in deep canyons with longer time for photochemistry to occur. Prevailing wind speeds also have a location-specific influence on concentration differences due to the shade. These difficulties suggest that one cannot simply use a proxy to simulate shading effects on street-canyon air quality. The relatively strong effect on street canyon ozone could also have implications for the production of Highly Oxidized Molecules (HOMs) and, hence, for new particle formation, but this requires further investigation with an extend chemistry scheme that includes the ozonolysis of alkenes and aromatics (e.g. Rissanen et al. (2014)) and is outside the scope of the present study.

Ultimately, the results above should be modelled in combination with effects on tracer transport, such as the impact of heating (e.g. Cai (2012b)) and enhanced wall roughness (e.g. in-canyon green infrastructures, Buccolieri et al. (2018)). Nevertheless, this study provides an initial quantification of shading effects on reactive air pollutants under various solar zenith angles, chemical schemes, traffic conditions, canyon geometry, and shading intensities. The findings provide steer for developing air quality models and proposing air quality solutions for urban hotspots. The technique utilised in this study is applicable for assessing the shading effects in the non-neutral atmosphere when pre-generated LES parameters are available to provide the dynamical input parameters, it allows a fast computation of a large number of scenarios without loss of sufficient spatial resolution and representation of transport, mixing, and chemical processes, and can be further expanded into a user friendly toolkit for street network air quality simulations.

Author statement

Yuqing Dai: Conceptualization, Methodology, Writing Original draft. **Xiaoming Cai**: Reviewing and Editing. **Jian Zhong**: Reviewing and Editing, Simulation Designment. **Andrea Mazzeo**: Reviewing and Editing. **Rob MacKenzie**: Supervision, Reviewing and Editing.

Declaration of competing interest

The authors declare that they have no known competing financial interests or personal relationships that could have appeared to influence the work reported in this paper.

Data availability

Data will be made available on request.

Acknowledgements

The authors would like to thank the University of Birmingham's BlueBEAR HPC service (http://www.bear.bham.ac.uk) for offering the computational resource. A.R.MK thanks funding support of the Natural Environment Research Council (grants NE/S013814/1, NE/S003487/1).

Appendix A. Supplementary data

Supplementary data to this article can be found online at https://doi.org/10.1016/j.envpol.2022.120347.

References

Abhijith, K., Kumar, P., Gallagher, J., McNabola, A., Baldauf, R., Pilla, F., Broderick, B., Di Sabatino, S., Pulvirenti, B., 2017. Air pollution abatement performances of green infrastructure in open road and built-up street canyon environments–A review. Atmos. Environ. 162, 71–86.

Ahmad, K., Khare, M., Chaudhry, K., 2005. Wind tunnel simulation studies on dispersion at urban street canyons and intersections—a review. J. Wind Eng. Ind. Aerod. 93, 697–717.

Anenberg, S.C., Henze, D.K., Tinney, V., Kinney, P.L., Raich, W., Fann, N., Malley, C.S., Roman, H., Lamsal, L., Duncan, B., 2018. Estimates of the global burden of ambient PM 2.5, ozone, and NO 2 on asthma incidence and emergency room visits. Environ. Health Perspect. 126, 107004.

Baik, J.-J., Kang, Y.-S., Kim, J.-J., 2007. Modeling reactive pollutant dispersion in an urban street canyon. Atmos. Environ. 41, 934–949.

Barlow, J.F., Harman, I.N., Belcher, S.E., 2004. Scalar fluxes from urban street canyons. Part I: laboratory simulation. Boundary-Layer Meteorol. 113, 369–385.

Bortier, K., De Temmerman, L., Ceulemans, R., 2000. Effects of ozone exposure in open-top chambers on poplar (Populus nigra) and beech (Fagus sylvatica): a comparison. Environ. Pollut. 109, 509–516.

Boulter, P., Barlow, T., Latham, S., McCrae, I., 2009. Emission Factors 2009: Report 1-a Review of Methods for Determining Hotexhaust Emission Factors for Road Vehicles. TRL Published Project Report.

Bourbia, F., Awbi, H., 2004. Building cluster and shading in urban canyon for hot dry climate: Part 2: shading simulations. Renew. Energy 29, 291–301.

Bright, V.B., Bloss, W.J., Cai, X., 2013. Urban street canyons: coupling dynamics, chemistry and within-canyon chemical processing of emissions. Atmos. Environ. 68, 127–142.

Buccolieri, R., Jeanjean, A.P., Gatto, E., Leigh, R.J., 2018. The impact of trees on street ventilation, NOx and PM2. 5 concentrations across heights in Marylebone Rd street canyon, central London. Sustain. Cities Soc. 41, 227–241.

Cai, X.-M., 2012a. Effects of wall heating on flow characteristics in a street canyon. Boundary-Layer Meteorol. 142, 443–467.

Cai, X., 2012b. Effects of differential wall heating in street canyons on dispersion and ventilation characteristics of a passive scalar. Atmos. Environ. 51, 268–277.

Carpenter, L., Clemitshaw, K., Burgess, R., Penkett, S., Cape, J., McFadyen, G., 1998. Investigation and evaluation of the NOx/O3 photochemical steady state. Atmos. Environ. 32, 3353–3365.

Carslaw, D.C., Beevers, S.D., 2004. Investigating the potential importance of primary NO2 emissions in a street canyon. Atmos. Environ. 38, 3585–3594.

Chatzidimitriou, A., Yannas, S., 2017. Street canyon design and improvement potential for urban open spaces; the influence of canyon aspect ratio and orientation on microclimate and outdoor comfort. Sustain. Cities Soc. 33, 85–101.

Chew, L.W., Aliabadi, A.A., Norford, L.K., 2018. Flows across high aspect ratio street canyons: Reynolds number independence revisited. Environ. Fluid Mech. 18, 1275–1291.

Colbeck, I., MacKenzie, A.R., 1994. Air Pollution by Photochemical Oxidants.

Dai, Y., Cai, X., Zhong, J., MacKenzie, A.R., 2021. Modelling Chemistry and Transport in Urban Street Canyons: Comparing Offline Multi-Box Models with Large-Eddy Simulation, 264. Atmospheric Environment, p. 118709.

Dai, Y., Cai, X., Zhong, J., MacKenzie, A.R., 2022. Street canyon NO2 "hotspots" and regulatory "wiggle room": the interacting effects of free-radical chemistry, canyon geometry, primary NO2, and emissions. npj Climate Atmos. Sci. Submitted for publication.

Finlayson-Pitts, B.J., Pitts Jr., J.N., 1999. Chemistry of the Upper and Lower Atmosphere: Theory, Experiments, and Applications. Elsevier.

Garmory, A., Kim, I., Britter, R., Mastorakos, E., 2009. Simulations of the dispersion of reactive pollutants in a street canyon, considering different chemical mechanisms and micromixing. Atmos. Environ. 43, 4670–4680.

Grawe, D., Cai, X.-M., Harrison, R.M., 2007. Large eddy simulation of shading effects on NO2 and O3 concentrations within an idealised street canyon. Atmos. Environ. 41, 7304–7314.

Gromke, C., Ruck, B., 2007. Influence of trees on the dispersion of pollutants in an urban street canyon—experimental investigation of the flow and concentration field. Atmos. Environ. 41, 3287–3302.

Hang, J., Chen, X., Chen, G., Chen, T., Lin, Y., Luo, Z., Zhang, X., Wang, Q., 2020. The influence of aspect ratios and wall heating conditions on flow and passive pollutant exposure in 2D typical street canyons. Build. Environ. 168, 106536.

Hood, C., Stocker, J., Seaton, M., Johnson, K., O'Neill, J., Thorne, L., Carruthers, D., 2021. Comprehensive evaluation of an advanced street canyon air pollution model. J. Air Waste Manag. Assoc. 71, 247–267.

Joint Air Quality Unit, 2017. Improving Air Quality in the UK: Tackling Nitrogen Dioxide in Our Towns and Cities. Department for Environment Food & Rural Affairs and Department for Transport, London, UK.

Kim, M.J., Park, R.J., Kim, J.-J., 2012. Urban air quality modeling with full O3–NOx–VOC chemistry: implications for O3 and PM air quality in a street canyon. Atmos. Environ. 47, 330–340.

Kwak, K.-H., Baik, J.-J., 2012. A CFD modeling study of the impacts of NOx and VOC emissions on reactive pollutant dispersion in and above a street canyon. Atmos. Environ. 46, 71–80.

Kwak, K.-H., Baik, J.-J., Lee, K.-Y., 2013. Dispersion and photochemical evolution of reactive pollutants in street canyons. Atmos. Environ. 70, 98–107.

Lee, J.D., Lewis, A.C., Monks, P.S., Jacob, M., Hamilton, J.F., Hopkins, J.R., Watson, N. M., Saxton, J.E., Ennis, C., Carpenter, L.J., 2006. Ozone photochemistry and elevated isoprene during the UK heatwave of August 2003. Atmos. Environ. 40, 7598–7613.

Li, C.W., Brasseur, G.P., Schmidt, H., Mellado, J.P., 2021. Error induced by neglecting subgrid chemical segregation due to inefficient turbulent mixing in regional chemical-transport models in urban environments. Atmos. Chem. Phys. 21, 483–503.

Li, N., He, Q., Greenberg, J., Guenther, A., Li, J., Cao, J., Wang, J., Liao, H., Wang, Q., Zhang, Q., 2018. Impacts of biogenic and anthropogenic emissions on summertime ozone formation in the Guanzhong Basin, China. Atmos. Chem. Phys. 18, 7489–7507.

Liu, J., Cui, S., Chen, G., Zhang, Y., Wang, X., Wang, Q., Gao, P., Hang, J., 2021. The influence of solar natural heating and NOx-O3 photochemistry on flow and reactive pollutant exposure in 2D street canyons. Sci. Total Environ. 759, 143527.

Monks, P.S., Archibald, A., Colette, A., Cooper, O., Coyle, M., Derwent, R., Fowler, D., Granier, C., Law, K.S., Mills, G., 2015. Tropospheric ozone and its precursors from the urban to the global scale from air quality to short-lived climate forcer. Atmos. Chem. Phys. 15, 8889–8973.

Morris, C., Simmonds, I., Plummer, N., 2001. Quantification of the influences of wind and cloud on the nocturnal urban heat island of a large city. J. Appl. Meteorol. Climatol. 40, 169–182.

Muilwijk, C., Schrijvers, P., Wuerz, S., Kenjereš, S., 2016. Simulations of photochemical smog formation in complex urban areas. Atmos. Environ. 147, 470–484.

Murena, F., Di Benedetto, A., D'Onofrio, M., Vitiello, G., 2011. Mass transfer velocity and momentum vertical exchange in simulated deep street canyons. Boundary-Layer Meteorol. 140, 125–142.

Murena, F., Favale, G., Vardoulakis, S., Solazzo, E., 2009. Modelling dispersion of traffic pollution in a deep street canyon: application of CFD and operational models. Atmos. Environ. 43, 2303–2311.

Murray, C.J., Aravkin, A.Y., Zheng, P., Abbafati, C., Abbas, K.M., Abbasi-Kangevari, M., Abd-Allah, F., Abdelalim, A., Abdollahi, M., Abdollahpour, I., 2020. Global burden of 87 risk factors in 204 countries and territories, 1990–2019: a systematic analysis for the Global Burden of Disease Study 2019. Lancet 396, 1223–1249.

Nations, U., 2018. Revision of World Urbanization Prospects, vol. 799. United Nations, New York, NY, USA.

Nilsson, T.M., Niklasson, G.A., 1995. Radiative cooling during the day: simulations and experiments on pigmented polyethylene cover foils. Sol. Energy Mater. Sol. Cell. 37, 93–118.

Paolini, R., Mainini, A.G., Poli, T., Vercesi, L., 2014. Assessment of thermal stress in a street canyon in pedestrian area with or without canopy shading. Energy Proc. 48, 1570–1575.
Park, S.-J., Kim, J.-J., Kim, M.J., Park, R.J., Cheong, H.-B., 2015. Characteristics of flow and reactive pollutant dispersion in urban street canyons. Atmos. Environ. 108, 20–31.
Pugh, T.A., MacKenzie, A.R., Whyatt, J.D., Hewitt, C.N., 2012. Effectiveness of green infrastructure for improvement of air quality in urban street canyons. Environ. Sci. Technol. 46, 7692–7699.
R Core Team, T., 2019. R: A Language and Environment for Statistical Computing. Vienna, Austria.
Rissanen, M.P., Kurten, T., Sipilä, M., Thornton, J.A., Kangasluoma, J., Sarnela, N., Junninen, H., Jørgensen, S., Schallhart, S., Kajos, M.K., 2014. The formation of highly oxidized multifunctional products in the ozonolysis of cyclohexene. J. Am. Chem. Soc. 136, 15596–15606.
Salmond, J., Williams, D., Laing, G., Kingham, S., Dirks, K., Longley, I., Henshaw, G., 2013. The influence of vegetation on the horizontal and vertical distribution of pollutants in a street canyon. Sci. Total Environ. 443, 287–298.
Satsangi, G.S., Lakhani, A., Kulshrestha, P., Taneja, A., 2004. Seasonal and diurnal variation of surface ozone and a preliminary analysis of exceedance of its critical levels at a semi-arid site in India. J. Atmos. Chem. 47, 271–286.
Saunders, S.M., Jenkin, M.E., Derwent, R., Pilling, M., 2003. Protocol for the development of the Master Chemical Mechanism, MCM v3 (Part A): tropospheric degradation of non-aromatic volatile organic compounds. Atmos. Chem. Phys. 3, 161–180.
Schlichting, H., Kestin, J., 1961. Boundary Layer Theory. Springer.
Seinfeld, J., Pandis, S., 2008. Atmospheric Chemistry and Physics, vol. 1997. New York.
Sillman, S., 1999. The relation between ozone, NOx and hydrocarbons in urban and polluted rural environments. Atmos. Environ. 33, 1821–1845.
Solazzo, E., Vardoulakis, S., Cai, X., 2011. A novel methodology for interpreting air quality measurements from urban streets using CFD modelling. Atmos. Environ. 45, 5230–5239.
Takano, Y., Moonen, P., 2013. On the influence of roof shape on flow and dispersion in an urban street canyon. J. Wind Eng. Ind. Aerod. 123, 107–120.
Vardoulakis, S., Fisher, B.E., Pericleous, K., Gonzalez-Flesca, N., 2003. Modelling air quality in street canyons: a review. Atmos. Environ. 37, 155–182.
Watson, L., Shallcross, D., Utembe, S., Jenkin, M., 2008. A Common Representative Intermediates (CRI) mechanism for VOC degradation. Part 2: gas phase mechanism reduction. Atmos. Environ. 42, 7196–7204.
Weng, Q., Fu, P., 2014. Modeling annual parameters of clear-sky land surface temperature variations and evaluating the impact of cloud cover using time series of Landsat TIR data. Rem. Sens. Environ. 140, 267–278.
Wu, L., Hang, J., Wang, X., Shao, M., Gong, C., 2021. APFoam 1.0: integrated computational fluid dynamics simulation of O 3–NO x–volatile organic compound chemistry and pollutant dispersion in a typical street canyon. Geosci. Model Dev. (GMD) 14, 4655–4681.
Yang, H., Chen, G., Wang, D., Hang, J., Li, Q., Wang, Q., 2021a. Influences of street aspect ratios and realistic solar heating on convective heat transfer and ventilation in full-scale 2D street canyons. Build. Environ. 204, 108125.
Yang, H., Chen, T., Lin, Y., Buccolieri, R., Mattsson, M., Zhang, M., Hang, J., Wang, Q., 2020. Integrated impacts of tree planting and street aspect ratios on CO dispersion and personal exposure in full-scale street canyons. Build. Environ. 169, 106529.
Yang, H., Lam, C.K.C., Lin, Y., Chen, L., Mattsson, M., Sandberg, M., Hayati, A., Claesson, L., Hang, J., 2021b. Numerical investigations of Re-independence and influence of wall heating on flow characteristics and ventilation in full-scale 2D street canyons. Build. Environ. 189, 107510.
Yazid, A.W.M., Sidik, N.A.C., Salim, S.M., Saqr, K.M., 2014. A review on the flow structure and pollutant dispersion in urban street canyons for urban planning strategies. Simulation 90, 892–916.
Zeng, W., Zhao, H., Liu, R., Yan, W., Qiu, Y., Yang, F., Shu, C., Zhan, Y., 2020. Association between NO2 cumulative exposure and influenza prevalence in mountainous regions: a case study from southwest China. Environ. Res. 189, 109926.
Zhong, J., Cai, X.-M., Bloss, W.J., 2014. Modelling segregation effects of heterogeneous emissions on ozone levels in idealised urban street canyons: using photochemical box models. Environ. Pollut. 188, 132–143.
Zhong, J., Cai, X.-M., Bloss, W.J., 2015. Modelling the dispersion and transport of reactive pollutants in a deep urban street canyon: using large-eddy simulation. Environ. Pollut. 200, 42–52.
Zhong, J., Cai, X.-M., Bloss, W.J., 2016a. Coupling dynamics and chemistry in the air pollution modelling of street canyons: a review. Environ. Pollut. 214, 690–704.
Zhong, J., Cai, X.-M., Bloss, W.J., 2016b. Modelling photochemical pollutants in a deep urban street canyon: application of a coupled two-box model approximation. Atmos. Environ. 143, 86–107.
Zhong, J., Cai, X.-M., Bloss, W.J., 2017. Large eddy simulation of reactive pollutants in a deep urban street canyon: coupling dynamics with O_3-NO_x-VOC chemistry. Environ. Pollut. 224, 171–184.
Zhong, J., Nikolova, I., Cai, X., MacKenzie, A.R., Harrison, R.M., 2018. Modelling traffic-induced multicomponent ultrafine particles in urban street canyon compartments: factors that inhibit mixing. Environ. Pollut. 238, 186–195.